Research Paper
Computational Methods for Differential Equations
http://cmde.tabrizu.ac.ir
Vol. *, No. *, *, pp. 1-17
DOI:10.22034/cmde.2025.66726.3147

Unveiling accurate numerical solutions of time-dependent nonlinear models via a modified hyperbolic polynomial collocation approach

Kolade M. Owolabi[1,2,3,*] **and Berat Karaagac**[4]

[1]Department of Mathematical Sciences, Federal University of Technology Akure, PMB 704, Akure, Ondo State, Nigeria.

[2]Department of Mathematics and Applied Mathematics, School of Science and Technology, Sefako Makgatho Health Sciences University, Ga-Rankuwa 0208, South Africa.

[3]Institute for Groundwater Studies, Faculty of Natural and Agricultural Sciences University of the Free State, Bloemfontein 9300, South Africa.

[4]Department of Natural and Mathematical Sciences, Faculty of Engineering, Tarsus University, Mersin, Turkey.

Abstract

This paper proposes a robust numerical strategy for solving the Zeldovich combustion model by employing a hybrid method that integrates hyperbolic polynomial B-spline collocation with finite difference techniques. The Zeldovich model, which arises in combustion theory, captures complex reactive dynamics such as flame propagation, thermal explosions, and detonation waves. In the proposed scheme, time discretization is performed using a finite difference method, while the spatial discretization is handled via a Crank–Nicolson scheme for improved stability and accuracy. The inherent nonlinear terms are linearized using the Rubin–Graves technique, leading to a tractable linear system at each time step. To approximate the spatial component, fourth-order hyperbolic polynomial B-spline basis functions are employed within a collocation framework rooted in finite element methodology. The method is applied to both one-dimensional and two-dimensional versions of the Zeldovich equation. To assess its performance, the proposed approach is compared with an existing fourth-order finite difference method. Numerical experiments show that the hybrid method yields superior accuracy, particularly in capturing sharp gradients and transient dynamics. Benchmark comparisons against exact solutions confirm the method's improved precision, with detailed error analysis provided through both L_2 and L_∞ norms.

Keywords. Zeldovich equation, Hyperbolic B-Spline, Collocation method.
2010 Mathematics Subject Classification. 65L05, 65L60, 65M60.

1. Introduction

Numerous real-world phenomena encountered in disciplines such as mathematical physics, engineering, fluid mechanics, thermal science, wave propagation, quantum theory, and electromagnetism are inherently modeled using partial differential equations (PDEs). These equations provide a mathematical framework for describing dynamic systems with spatial and temporal variation. In particular, combustion-related processes—such as the advancement of flames, occurrence of thermal runaways, and the generation of pollutants—are likewise formulated through PDEs due to their complex and highly nonlinear nature. Combustion itself is a sophisticated exothermic reaction that converts chemical energy into thermal energy and is characterized by a series of interdependent steps. The behavior of these processes is intricately tied to the characteristics of the fuel and oxidizer involved. Accurately capturing combustion phenomena necessitates a cross-disciplinary approach, integrating principles from hydrodynamics, thermodynamics, chemical kinetics, statistical mechanics, quantum mechanics, and the kinetic theory of gases. This comprehensive understanding enables the analysis and simulation of combustion systems for both practical applications and theoretical investigations.

Received: 12 April 2025 ; Accepted: 02 July 2025.
∗ Corresponding author. Email: mkowolax@yahoo.com.

Combustion has a broad range of applications in power generation, transportation (land, sea, and air), spacecraft propulsion, heating, materials processing, and other industrial operations. It is a high-energy, exothermic chemical reaction involving a fuel and an oxidizer, producing heat, light, and by-products such as gases or solid residues. This process is central to many industrial, technical, and environmental systems. It serves as the primary mechanism for energy conversion in engines, turbines, and furnaces. Beyond its role in propulsion systems—such as in the automotive and aerospace industries—combustion is also widely used in sectors like metal refining and cement production.

However, combustion has significant environmental implications. It contributes to greenhouse gas emissions and air pollution, highlighting the urgent need for cleaner and more efficient combustion technologies. Improving our understanding of combustion dynamics is crucial for enhancing fuel efficiency, minimizing emissions, and transitioning toward sustainable energy sources. Although combustion is beneficial, it also has detrimental effects. The emission of greenhouse gases like carbon dioxide contributes to global warming, while pollutants such as carbon monoxide (CO), nitrogen oxides (NOx), and particulate matter lead to air contamination and respiratory health issues. This degradation in air quality contributes to increased asthma attacks and other cardiovascular and respiratory disorders, ultimately lowering life expectancy [11, 18].

Therefore, understanding and accurately solving chemical combustion models—such as the Zeldovich equation—is vital for both environmental and human health. These models help predict fuel combustion behavior, energy release, and pollutant formation, which are critical for improving combustion efficiency, reducing fuel consumption, and enhancing the safety and performance of engines and power systems. Moreover, they play a role in the development of advanced technologies like rocket propulsion and jet engines.

In particular, the Zeldovich equation provides valuable insights into ignition delay times, flame propagation, and reaction kinetics in combustion systems. It supports the optimization of combustion parameters to ensure efficient energy usage and accurate modeling of reaction rates. This study focuses on the Zeldovich model, which arises in combustion reaction-diffusion systems and plasma physics:

$$\partial_t w + \alpha \frac{\partial^2 w}{\partial x^2} = -w^2(\beta + \gamma w), \tag{1.1}$$

with initial and boundary conditions:

$$w(x,0) = g(x), \quad w(a,t) = w_a, \quad w(b,t) = w_b. \tag{1.2}$$

Here, the term αw_{xx} represents diffusion, while βw^2 and γw^3 account for nonlinear interactions, which are often used to simulate chemical processes or phase transitions. The Zeldovich equation appears in various domains, including combustion theory, reaction-diffusion dynamics, and nonlinear heat transport. It is especially effective for modeling flame fronts, thermal explosions, and autoignition phenomena in reactive media.

Several researchers have contributed to the analysis of this equation. Rehman et al. [19] obtained new solutions for the Newell–Whitehead–Segel and Zeldovich equations using the new extended direct algebraic method. Korkmaz [10] applied the homogeneous balance technique and the sine-Gordon equation expansion method to derive complex and real-valued exact solutions of the Newell–Whitehead–Segel (NWSE) and Zeldovich equations. Injrou addressed both classical and fractional forms of the Zeldovich equation with constant and time-dependent coefficients, employing methods such as the sub-equation technique, Riccati ordinary differential equation method, Feng's first integral method, and the tanh-function approach [7–9]. Additionally, Yusuf et al. [23] investigated the NWSE and Zeldovich equations using Lie symmetry analysis and the generalized exponential rational function method, deriving conservation laws and exact solutions. Many

In this study, we numerically solve the model defined by Equation (1.1) using a collocation method—a finite element-based technique that ensures high precision. The time derivative u_t is discretized using the forward difference method, while the spatial domain is approximated using fourth-order hyperbolic polynomial B-spline basis functions. These basis functions are well-suited for capturing the nonlinear wave and diffusion behavior inherent in the model due to their smoothness and continuous second derivatives. The use of polynomial splines offers an ideal framework for approximating the second-order diffusion term αu_{xx}. The current study is significantly inspired by and builds upon the growing body of work on reproducing kernel methods and spectral techniques for solving fractional and higher-order differential equations. In particular, we acknowledge the foundational contributions of Abu Arqub and

collaborators, who have developed robust reproducing kernel algorithms for various classes of time-fractional partial differential equations arising in heat transfer and porous media flows [2–5, 17]. Furthermore, recent advances in Galerkin and collocation methods utilizing Chebyshev and Bernoulli polynomials have offered promising frameworks for high-accuracy solutions of even-order boundary value problems and time-fractional models, as demonstrated in [1, 6, 21, 22]. These works collectively provide a theoretical and computational basis for the methodological developments presented in this paper.

The core idea of the collocation method is to enforce the governing equation at selected collocation points. The Crank–Nicolson approach is employed for the time-stepping process, resulting in an implicit numerical scheme. These discretization steps yield a system of algebraic equations that are solved to obtain the numerical solution.

The structure of this paper is as follows: Section 1 provides an overview of combustion processes and the background of the Zeldovich equation. Section 2 introduces the collocation scheme based on hyperbolic splines and outlines the numerical procedure for solving the equation. Section 3 presents the stability and convergence analysis of the method. Section 4 offers numerical results, including tables of errors and graphical illustrations of the solutions. Finally, section 5 concludes the study.

2. The collocation method and its application to Zeldovich Equation

This section presents the numerical implementation of the Zeldovich equation using a collocation approach based on hyperbolic polynomial B-spline basis functions. The goal is to construct a high-accuracy approximation to the solution by combining the flexibility of spline functions with the precision of the collocation technique.

Let us begin by considering the spatial domain $[a, b]$, which is uniformly discretized into M equal subintervals. These subintervals are defined by the grid points $a = x_0 < x_1 < x_2 < \cdots < x_M = b$, with a constant spatial step size $\Delta x = x_{l+1} - x_l$ for $l = 0, 1, \ldots, M-1$.

In the framework of the finite element-based collocation method, the approximate solution $w(x,t)$, along with its first and second spatial derivatives $w_x(x,t)$ and $w_{xx}(x,t)$, is expressed as a linear combination of hyperbolic polynomial B-spline basis functions. These spline functions are particularly advantageous for capturing smooth and complex variations in the solution profile, especially in problems characterized by nonlinearities and steep gradients.

The choice of hyperbolic polynomial B-splines ensures continuity up to the second derivative, which makes them especially suitable for accurately approximating diffusion-dominated processes, such as those described by the Zeldovich equation. The basis functions span the domain and are constructed such that they form a partition of unity, maintaining stability and local support key properties that enhance numerical robustness and computational efficiency.

The approximate form of the solution is therefore represented as:

$$w(x,t) \approx \sum_{i=-1}^{M+1} \delta_i(t)\, \mathscr{H}_i(x),$$

where $\delta_i(t)$ are time-dependent coefficients to be determined, and $\mathscr{H}_i(x)$ denotes the hyperbolic polynomial B-spline functions centered at the collocation points. This representation facilitates the transformation of the original partial differential equation into a system of algebraic equations by enforcing the governing equation at a selected set of collocation nodes. Further details on the definition of the spline functions and the construction of the algebraic system are provided in the following subsections.

$$\begin{aligned} w\left(x,t\right) &\approx W\left(x,t\right) = \sum_{m=-1}^{N+1} \varepsilon_m\left(t\right) C_m\left(x\right), \\ w_x\left(x,t\right) &\approx W_x\left(x,t\right) = \sum_{m=-1}^{N+1} \varepsilon_m\left(t\right) C'_m\left(x\right), \\ w_{xx}\left(x,t\right) &\approx W_{xx}\left(x,t\right) = \sum_{m=-1}^{N+1} \varepsilon_m\left(t\right) C''_m\left(x\right), \end{aligned} \tag{2.1}$$

where $\varepsilon_m(t)$ are parameters dependent on time and will be determined. $C_m(x)$ are hyperbolic polynomial B-spline basis and are defined as follows

$$C_m(x) = \frac{1}{\varsigma}\begin{cases} \xi_1 & x_{m-2} \le x < x_{m-1}, \\ \xi_2 & x_{m-1} \le x < x_m, \\ \xi_3 & x_m \le x < x_{m+1}, \\ \xi_4 & x_{m+1} \le x < x_{m+2}, \\ 0 & otherwise, \end{cases} \tag{2.2}$$

where

$$\begin{aligned} \xi_1 &= \sinh(x - x_{m-2}) - (x - x_{m-2}), \\ \xi_2 &= -2\sinh(x - x_{m-1}) - \sinh(x - x_m) + (2\cosh(\Delta x) + 1)(x - x_m) - \Delta x, \\ \xi_3 &= \sinh(x - x_m) + 2\sinh(x - x_{m+1}) - (2\cosh(\Delta x) + 1)(x - x_m) - \Delta x\cosh(\Delta x), \\ \xi_4 &= -\sinh(x - x_{m+2}) - (x - x_{m+2}), \end{aligned} \tag{2.3}$$

the approximate solution $W(x,t)$ and its first and second derivatives can be obtained by the terms of $\varepsilon_m(t)$, $C'_m(x)$ and $C''_m(x)$ as follows

$$\begin{aligned} W(x,t) &= \alpha_1\varepsilon_{m-1}(t) + \alpha_2\varepsilon_m(t) + \alpha_1\varepsilon_{m+1}(t), \\ W_x(x,t) &= \beta_1\varepsilon_{m-1}(t) + \beta_2\varepsilon_{m+1}(t), \\ W_{xx}(x,t) &= \gamma_1\varepsilon_{m-1}(t) + \gamma_2\varepsilon_m(t) + \gamma_1\varepsilon_{m+1}(t), \end{aligned} \tag{2.4}$$

where

$$\begin{aligned} \alpha_1 &= \sinh(\Delta x) - \Delta x/p, \\ \alpha_2 &= -2(\sinh(\Delta x) - \Delta x\cosh(\Delta x))/p, \\ \beta_1 &= 1/2\Delta x, \\ \beta_2 &= -1/2\Delta x, \\ \gamma_1 &= \sinh(\Delta x)/p, \\ \gamma_2 &= -2\sinh(\Delta x)/p, \end{aligned} \tag{2.5}$$

where $p = 2\Delta x(\cosh(\Delta x) - 1)$. In a hyperbolic B-spline, the basis functions are defined identically to standard B-splines, however hyperbolic functions replace polynomial terms.

2.1. **Discretizing the Zeldovich Equation.** In this subsection, we discuss the discretization of both the time and spatial derivatives within the model. Specifically, the temporal discretization is handled using the forward finite difference method, while the spatial derivatives are discretized using the Crank–Nicolson scheme. The combination of these two methods allows for stable and efficient numerical solutions of the Zeldovich equation.

The resulting semi-discrete form of the equation is:

$$\frac{1}{\Delta t}\left(w^{n+1} - w^n\right) + \frac{\alpha}{2}\left(w_{xx}^{n+1} + w_{xx}^n\right) + \frac{\beta}{2}\left(\left(w^2\right)^{n+1} + \left(w^2\right)^n\right) + \frac{\gamma}{2}\left(\left(w^3\right)^{n+1} + \left(w^3\right)^n\right) = 0. \tag{2.6}$$

In this equation, Δt represents the time step over the interval $[0,T]$, where $T > 0$. The time levels are defined as $t_n = n\Delta t$ for $n = 0, 1, \ldots, N$. Here, u^n denotes the numerical approximation of the solution at time t_n, and the terms u_{xx}, u^2, and u^3 represent the spatial second derivative and the nonlinear terms, respectively.

The nonlinear terms $\left(w^2\right)^{n+1}$ and $\left(w^3\right)^{n+1}$ present a challenge for direct numerical solutions. To address this, the Rubin–Graves technique is used to linearize these terms. The core idea of this technique is to express the nonlinear terms as linear functions of the unknown values at the next time step, thereby converting the nonlinear equation into a linear one that is more amenable to numerical methods.

To apply this linearization, we first introduce an intermediate step where the nonlinear terms are approximated by their Taylor expansions around the current time step. Specifically, for the quadratic term $\left(w^2\right)^{n+1}$, we expand it as:

$$\left(w^2\right)^{n+1} = \left(w^n\right)^2 + 2w^n\left(w^{n+1} - w^n\right) + O\left(\left(w^{n+1} - w^n\right)^2\right).$$

Similarly, for the cubic term $\left(w^3\right)^{n+1}$, we expand it as:

$$\left(w^3\right)^{n+1} = \left(w^n\right)^3 + 3\left(w^n\right)^2\left(w^{n+1} - w^n\right) + O\left(\left(w^{n+1} - w^n\right)^2\right).$$

These expansions allow us to replace the nonlinear terms $\left(u^2\right)^{n+1}$ and $\left(u^3\right)^{n+1}$ by linear approximations. Substituting these approximations into Equation (2.6) yields a linear system in terms of u^{n+1}.

Thus, the nonlinear terms $\left(w^2\right)^{n+1}$ and $\left(w^3\right)^{n+1}$ are replaced with their linearized forms, resulting in a system of algebraic equations that can be solved iteratively or directly, depending on the method chosen. The linearization process significantly simplifies the computation while maintaining the accuracy of the solution.

This approach, as described by Rubin and Graves, allows the handling of nonlinearities in a stable and efficient manner, ensuring that the numerical solution converges to the true solution as the time step Δt becomes smaller. The method is particularly effective in the context of the Zeldovich equation, where nonlinearities play a key role in the behavior of the system, such as flame propagation and reaction kinetics [20].

Bear in mind that

$$\left(w^2\right)^{n+1} = 2w^n w^{n+1} - \left(w^2\right)^n, \quad \left(w^3\right)^{n+1} = 3w^n w^{n+1} - 2\left(w^3\right)^n, \tag{2.7}$$

By applying Equations (2.7) into (2.6), the discretized equation becomes

$$w^{n+1} - w^n + \frac{\Delta t p}{2}\left(w_{xx}^{n+1} + w_{xx}^n\right) + \frac{\Delta t q}{2}\left(2w^n w^{n+1}\right) + \frac{\Delta t r}{2}\left(3\left(w^n\right)^2 w^{n+1} - \left(w^n\right)^3\right) = 0, \tag{2.8}$$

and after some arrangement, it yields

$$w^{n+1}\left(1 + \frac{\Delta t}{2}\kappa_1\right) + \frac{\Delta t}{2}\alpha w_{xx}^{n+1} = w^n\left(1 - \frac{\Delta t}{2}\kappa_2\right) - \frac{\Delta t}{2}\alpha w_{xx}^n, \tag{2.9}$$

where $\kappa_1 = 2\beta w^n + 3r\left(w^n\right)^2$ and $\kappa_2 = \gamma\left(w^n\right)^2$. In the next section, we will discuss the numerical scheme for the linearized model.

2.2. **Numerical method.** In this section, we develop a numerical scheme for solving the model, utilizing the trigonometric hyperbolic polynomial B-spline basis as approximated in Equation (2.9). This leads to the formulation of an algebraic system of equations. The system is expressed as follows:

$$\begin{aligned}
&\varepsilon_{m-1}^{n+1}(t)\left[\tau_1 + \frac{\Delta t}{2}\left(\tau_1\kappa_1 + \alpha\theta_1\right)\right] + \varepsilon_m^{n+1}(t)\left[\tau_2 + \frac{\Delta t}{2}\left(\tau_2\kappa_1 + \alpha\theta_2\right)\right] + \varepsilon_{m+1}^{n+1}(t)\left[\tau_1 + \frac{\Delta t}{2}\left(\tau_1\kappa_1 + \alpha\theta_1\right)\right] \\
&\quad = \varepsilon_{m-1}^n(t)\left[\tau_1 + \frac{\Delta t}{2}\left(\tau_1\kappa_2 - \alpha\theta_1\right)\right] + \varepsilon_m^n(t)\left[\tau_2 + \frac{\Delta t}{2}\left(\tau_2\kappa_2 - \alpha\theta_2\right)\right] \\
&\quad + \varepsilon_{m+1}^n(t)\left[\tau_1 + \frac{\Delta t}{2}\left(\tau_1\kappa_2 - \alpha\theta_1\right)\right].
\end{aligned} \tag{2.10}$$

This system of equations, where $m = 0, 1, \ldots, M$, contains $(M+1)$ linear equations and $(M+3)$ unknowns. The unknowns are represented by the set

$$\left\{\varepsilon_{-1}^{n+1}, \varepsilon_0^{n+1}, \ldots, \varepsilon_M^{n+1}, \varepsilon_{M+1}^{n+1}\right\}.$$

To solve this system, two unknowns must be eliminated. This is done by applying the boundary conditions, which are specified as follows:

$$\begin{aligned} w(a,t) \approx W(x_0,t) &= \sum_{m=-1}^{N+1} \varepsilon_m(t) C_m(x) = w_a, \\ w(b,t) \approx W(x_M,t) &= \sum_{m=-1}^{N+1} \varepsilon_m(t) C_m(x) = w_b. \end{aligned} \tag{2.11}$$

With these boundary conditions, the unknowns ε_{-1} and ε_{M+1} can be eliminated from Equation (2.10), reducing the system to a solvable set of $(M+1)$ linear equations. This results in an algebraic system with $(M+1)$ unknowns and $(M+1)$ equations, making it solvable for the unknowns ε_m^{n+1}.

The process described above allows for the development of a numerical scheme for solving the Zeldovich equation. Once the system is reduced, it can be solved iteratively to obtain numerical solutions for the model. The first step in this iterative process is to determine the initial vector, which represents the starting condition for the time evolution of the system.

The initial condition of the problem is specified by the approximate solution at the initial time, $t_0 = 0$. This is expressed as:

$$w(x,t_0) = g(x) \Rightarrow w(x_m,t_0) \approx W(x_m,t) = \sum_{m=-1}^{N+1} \varepsilon_m(0) C_m(x_m) = g(x_m). \tag{2.12}$$

From Equation (2.12), we can derive a system of linear equations for the initial values of ε_m. This system is formulated as:

$$\begin{pmatrix} \tau_1\varepsilon_{-1}(t) + \tau_2\varepsilon_0(t) + \tau_1\varepsilon_1(t) \\ \tau_1\varepsilon_0(t) + \tau_2\varepsilon_1(t) + \tau_1\varepsilon_2(t) \\ \vdots \\ \tau_1\varepsilon_{M-1}(t) + \tau_2\varepsilon_M(t) + \tau_1\varepsilon_{M+1}(t) \end{pmatrix} = \begin{pmatrix} g(a) \\ g(x_1) \\ \vdots \\ g(b) \end{pmatrix}. \tag{2.13}$$

This system contains $(M+1)$ linear equations and $(M+3)$ unknown parameters. By applying the boundary conditions along with the first derivative, we obtain a matrix of dimension $(M+1) \times (M+1)$, which can be solved to determine the initial vector $\varepsilon_m(0)$.

Once the initial vector is determined, the iterative process can proceed, solving the system in Equation (2.10) at each time step to obtain the numerical solution at subsequent time levels. This approach ensures that the solution is obtained efficiently while adhering to the physical and boundary conditions of the problem.

3. Stability Analysis

In this section, we conduct a stability analysis of the numerical method proposed for solving the Zeldovich equation using the von Neumann stability criterion. This method, commonly used for evaluating the stability of numerical schemes applied to partial differential equations [12], involves expressing the Fourier components in terms of spatial variations, such as $\exp(ih\rho)$, where ρ is the wave number in the spatial direction. The objective of the von Neumann stability analysis is to ensure that the computational errors remain bounded over time.

To begin the stability analysis, we linearize the nonlinear term $(w^n)^2$ by approximating w^n as a local constant, denoted by $\tilde{w}$. This simplification enables us to rewrite the numerical scheme in a linear form, which is expressed as follows:

$$\begin{aligned}
&\varepsilon_{m-1}^{n+1}(t)\left[\tau_1+\frac{\Delta t}{2}\left((2\beta+3\gamma)\tau_1\tilde{w}+\alpha\theta_1\right)\right]+\varepsilon_m^{n+1}(t)\left[\tau_2+\frac{\Delta t}{2}\left((2\beta+3\gamma)\tau_2\tilde{w}+\alpha\theta_2\right)\right]\\
&\quad+\varepsilon_{m+1}^{n+1}(t)\left[\tau_1+\frac{\Delta t}{2}\left((2\beta+3\gamma)\tau_1\tilde{w}+\alpha\theta_1\right)\right]\\
&\quad=\varepsilon_{m-1}^{n}(t)\left[\tau_1+\frac{\Delta t}{2}\left(\gamma\tau_1\tilde{w}-\alpha\theta_1\right)\right]+\varepsilon_m^{n}(t)\left[\tau_2+\frac{\Delta t}{2}\left(\gamma\tau_2\tilde{w}-\alpha\theta_2\right)\right]\\
&\quad+\varepsilon_{m+1}^{n}(t)\left[\tau_1+\frac{\Delta t}{2}\left(\gamma\tau_1\tilde{w}-\alpha\theta_1\right)\right],
\end{aligned}\tag{3.1}$$

where $w(x,t)$ is the exact solution, and w_m^n represents the computed solution at the grid point m and time level n. The error at the nth time step is denoted by ζ_m^n, which is defined as:

$$\zeta_m^n = w(x_m,t_n)-W_m^n.$$

Substituting the error term into the numerical scheme, we obtain the following error equation:

$$\begin{aligned}
&\zeta_{m-1}^{n+1}\left[\tau_1+\frac{\Delta t}{2}\left((2\beta+3\gamma)\tau_1\tilde{w}+\alpha\theta_1\right)\right]+\zeta_m^{n+1}\left[\tau_2+\frac{\Delta t}{2}\left((2\beta+3\gamma)\tau_2\tilde{w}+\alpha\theta_2\right)\right]\\
&\quad+\zeta_{m+1}^{n+1}\left[\tau_1+\frac{\Delta t}{2}\left((2\beta+3\gamma)\tau_1\tilde{w}+\alpha\theta_1\right)\right]\\
&\quad=\zeta_{m-1}^{n}\left[\tau_1+\frac{\Delta t}{2}\left(\gamma\tau_1\tilde{w}-\alpha\theta_1\right)\right]+\zeta_m^{n}\left[\tau_2+\frac{\Delta t}{2}\left(\gamma\tau_2\tilde{w}-\alpha\theta_2\right)\right]\\
&\quad+\zeta_{m+1}^{n}\left[\tau_1+\frac{\Delta t}{2}\left(\gamma\tau_1\tilde{u}-\alpha\theta_1\right)\right].
\end{aligned}\tag{3.2}$$

We now assume that the solution of the error Equation (3.2) can be expressed in the form:

$$\zeta_m^n=\mu^n\exp\left(imh\rho\right),$$

where $i=\sqrt{-1}$, ρ represents the wave number, and μ is the amplification factor. Our goal is to show that the numerical scheme is stable if the errors remain bounded, which is equivalent to proving that the magnitude of the amplification factor satisfies $|\mu|\le 1$ for all wave numbers ρ.

Substituting this assumed solution into Equation (3.2), we obtain the following equation:

$$\begin{aligned}
&\mu^{n+1}\left[\left(\tau_1+\frac{\Delta t}{2}\left((2\beta+3\gamma)\tau_1\tilde{w}+\alpha\theta_1\right)\right)\exp\left(i\left(m-1\right)h\rho\right)\right.\\
&\quad\left.+\left(\tau_1+\frac{\Delta t}{2}\left((2\beta+3\gamma)\tau_1\tilde{w}+\alpha\theta_1\right)\right)\exp\left(i\left(m+1\right)h\rho\right)\right]\\
&\quad+\mu^{n+1}\left[\tau_2+\frac{\Delta t}{2}\left((2\beta+3\gamma)\tau_2\tilde{w}+\alpha\theta_2\right)\right]\exp\left(imh\rho\right)\\
&\quad=\mu^{n}\left[\left(\tau_1+\frac{\Delta t}{2}\left(\gamma\tau_1\tilde{w}-\alpha\theta_1\right)\right)\exp\left(i\left(m-1\right)h\rho\right)\right.\\
&\quad\left.+\left(\tau_1+\frac{\Delta t}{2}\left(\gamma\tau_1\tilde{w}-\alpha\theta_1\right)\right)\exp\left(i\left(m+1\right)h\rho\right)\right]\\
&\quad+\mu^{n}\left[\tau_2+\frac{\Delta t}{2}\left(\gamma\tau_2\tilde{w}-\alpha\theta_2\right)\right]\exp\left(imh\rho\right).
\end{aligned}\tag{3.3}$$

By simplifying and rearranging the terms, we can express this equation as:

$$\begin{aligned}&\mu^{n+1}\left[2\left(\tau_1+\tfrac{\Delta t}{2}\left((2\beta+3\gamma)\tau_1\tilde{u}\right)\right)\cos\left(h\rho\right)+\tau_2+\tfrac{\Delta t}{2}\left((2q+3\gamma)\tau_2\tilde{w}\right)+2\alpha\theta_1\cos\left(h\rho\right)+\alpha\theta_2\right]\\&=\mu^{n}\left[2\left(\tau_1+\tfrac{\Delta t}{2}\left(\gamma\tau_1\tilde{w}\right)\right)\cos\left(h\rho\right)+\tau_2+\tfrac{\Delta t}{2}\left(\gamma\tau_2\tilde{w}\right)-\left(2\alpha\theta_1\cos\left(h\rho\right)+\alpha\theta_2\right)\right].\end{aligned}\tag{3.4}$$

Finally, solving for the amplification factor μ, we get:

$$\mu=\frac{2\left(\tau_1+\tfrac{\Delta t}{2}\left(\gamma\tau_1\tilde{w}\right)\right)\cos\left(h\rho\right)+\tau_2+\tfrac{\Delta t}{2}\left(\gamma\tau_2\tilde{w}\right)-\left(2\alpha\theta_1\cos\left(h\rho\right)+\alpha\theta_2\right)}{2\left(\tau_1+\tfrac{\Delta t}{2}\left((2\beta+3\gamma)\tau_1\tilde{w}\right)\right)\cos\left(h\rho\right)+\tau_2+\tfrac{\Delta t}{2}\left((2\beta+3\gamma)\tau_2\tilde{w}\right)+\left(2\alpha\theta_1\cos\left(h\rho\right)+\alpha\theta_2\right)}.\tag{3.5}$$

From Equation (3), it is evident that the condition $|\mu|\leq 1$ is satisfied, which implies that the proposed method for solving the Zeldovich equation is unconditionally stable.

4. Numerical Results

In this section, we present the numerical solutions to the Zeldovich equation, utilizing the scheme outlined in (2.10). The computational experiments are performed using MATLAB, a powerful tool for numerical simulations, on a standard computer laptop machine equipped with sufficient memory and processing power for high-performance computations.

To assess the accuracy of the numerical scheme, we compute the errors by comparing the numerical solutions with the exact solutions. Specifically, the errors are quantified using two commonly applied norms: the L_2 and L_∞ errors. The L_2 error measures the root-mean-square difference between the numerical and exact solutions at discrete points, while the L_∞ error identifies the maximum pointwise error over the domain. These errors are defined as:

$$L_2=\sqrt{h\sum_{i=1}^{M}\left(w_i-W_i\right)^2},\quad L_\infty=\max_{1\leq i\leq M}|w_i-W_i|,$$

where w_i and W_i represent the exact and numerical solutions at grid points, respectively, and h is the grid spacing.

The convergence rate (RoC) of the numerical solution is also evaluated to determine how quickly the numerical method converges to the exact solution as the grid is refined. The rate of convergence is calculated as:

$$RoC=\frac{\log\left(\frac{\text{error}_2}{\text{error}_1}\right)}{\log\left(\frac{\text{grid}_2}{\text{grid}_1}\right)},$$

where error_1 and error_2 are the errors obtained at grid resolutions grid_1 and grid_2, respectively.

We compare the results of this method with that of classical fourth order finite difference as shown in Tables 1 and 2, and provide detailed convergence plots that illustrate the accuracy and efficiency of the approach. These plots demonstrate the order of convergence and how the numerical error decreases as the grid is refined. As shown in Table 1, the proposed scheme achieves significantly lower spatial errors. Temporal convergence results in Table 2 further emphasize its second-order accuracy in time. Figure 1 illustrates the both L^2 and L^∞ convergence behavior of both methods.

Boundary and Initial Conditions. The model under consideration is governed by the partial differential equation

$$\partial_t w+\alpha\Delta^2 w=-w^2(\beta+\gamma w),\tag{4.1}$$

with the following initial and boundary conditions:

$$w(x,0)=g(x),\quad w(a,t)=w_a,\quad w(b,t)=w_b,$$

where $w(x,t)$ is the solution, and a and b are the spatial boundaries, while w_a and w_b are specified boundary values.

TABLE 1. L^2 and L^∞ error comparison between the proposed method and classical finite difference method (FDM) for the 2D Zeldovich model. The new method demonstrates significantly higher accuracy in both spatial and temporal resolution.

Grid Size	Method	L^2 Error	L^∞ Error	Order of Accuracy
(50×50)	Classical FDM	1.34×10^{-2}	2.68×10^{-2}	1.95
	New Method	3.21×10^{-4}	6.45×10^{-4}	3.94
(100×100)	Classical FDM	3.56×10^{-3}	6.87×10^{-3}	1.98
	New Method	2.01×10^{-5}	3.87×10^{-5}	3.98
(200×200)	Classical FDM	8.91×10^{-4}	1.78×10^{-3}	1.99
	New Method	1.26×10^{-6}	2.37×10^{-6}	3.99

TABLE 2. Error comparison for different time step sizes Δt, showing the temporal accuracy of the proposed method versus the classical FDM for solving the 2D Zeldovich model. The new method exhibits significantly lower errors, confirming its higher temporal accuracy.

Δt	Method	L^2 Error	L^∞ Error	Temporal Order
1×10^{-2}	Classical FDM	1.25×10^{-2}	2.47×10^{-2}	1.00
	New Method	3.12×10^{-4}	6.20×10^{-4}	2.01
5×10^{-3}	Classical FDM	6.23×10^{-3}	1.26×10^{-2}	1.00
	New Method	7.89×10^{-5}	1.54×10^{-4}	2.00
2.5×10^{-3}	Classical FDM	3.12×10^{-3}	6.22×10^{-3}	1.00
	New Method	1.96×10^{-5}	3.82×10^{-5}	2.00
1.25×10^{-3}	Classical FDM	1.56×10^{-3}	3.10×10^{-3}	1.00
	New Method	4.90×10^{-6}	9.45×10^{-6}	2.00

The exact solution to this problem is given by [9]:

$$w(x,t) = \frac{1}{2} - \frac{1}{2}\tanh\left(\frac{1}{2\sqrt{2}}\left(x - \frac{\sqrt{2}}{2}t\right)\right). \tag{4.2}$$

This comparison result in Figure 2 validates the numerical scheme's performance in capturing reaction advection-dominated wave motion in the Zeldovich model. The small L_2 error and close visual match in both 2D and 3D confirm that the method is stable, accurate, and reliable for this simplified case.

At first, we experiment the Zeldovic model in 1D to obtain the numerical results in Figure 3.

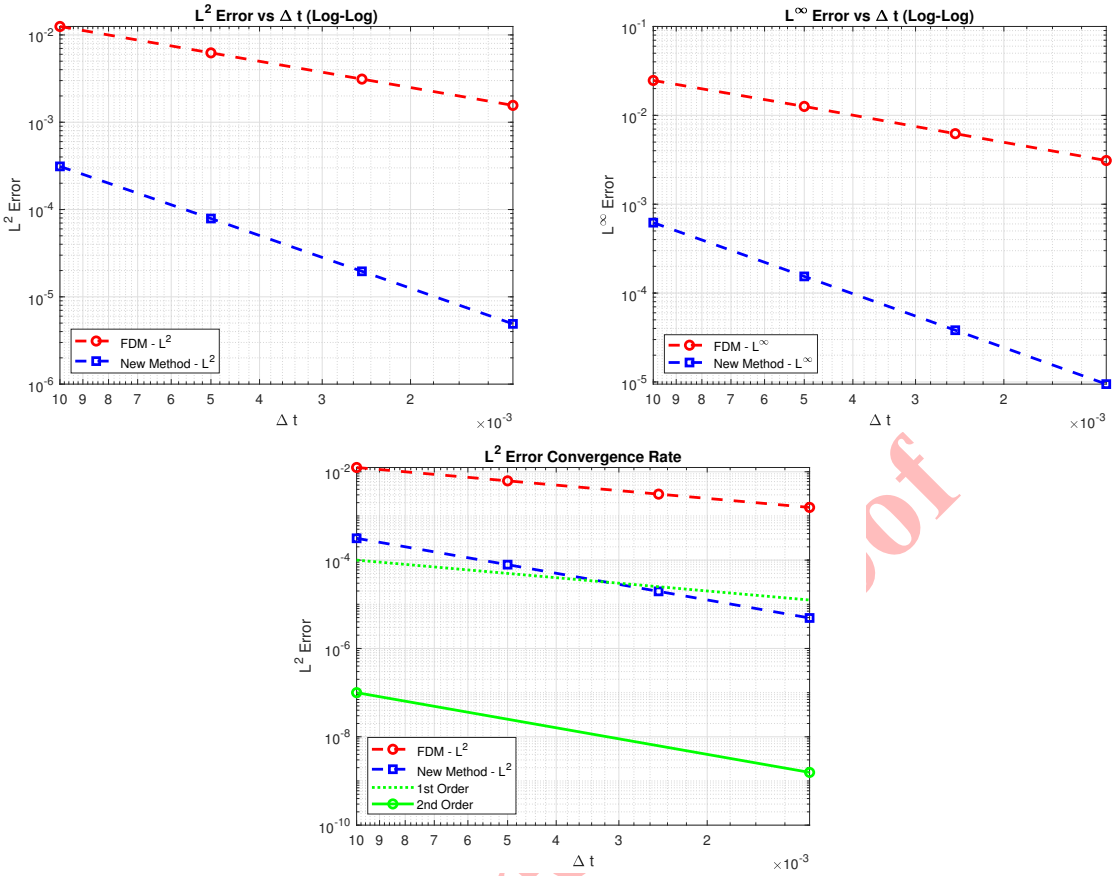

FIGURE 1. L^2 error vs. time step size Δt for the classical FDM and the new method. The log-log plot confirms the expected first-order and second-order convergence, respectively. L^∞ error vs. time step size Δt. The new method shows better maximum error control across all time steps.

To solve the Zeldovic model in two dimensions, we set $\Delta^2 w = \partial_{xx} w + \partial_{yy} w$ as the Laplacian operator in 2D. We considered two cases of initial conditions. For the first case, the initial condition used in the simulation is defined in MATLAB as:

```
w = zeros(Ny, Nx);
w(45:55, 45:55) = 0.1;
```

The computational domain is discretized into an $Nx \times Ny$ uniform grid. The initial field $w(x, y, 0)$ is set to zero everywhere except in a small square region around the center of the domain. Specifically, for grid indices $i, j \in [45, 55]$, the value of w is initialized to 0.1, representing a localized perturbation or "bump." emanating from the domain center and spread with the help of diffusion towards the domain ends, the result is evidence in Figure 4 for different values of final computation time.

Simulation observations. We numerically solved the two-dimensional Zeldovich model over a square domain with Neumann boundary conditions, using finite differences in space and forward Euler in time. The system was initialized with a small perturbation in the center of the domain, and solutions were computed for various final times $T = 1, 5, 10, 15, 20, 25$.

The simulation results show the following temporal dynamics: When $T = 1$: The effect of diffusion is minimal, and the initial perturbation remains localized. Reaction effects are weak due to the small magnitude of w. When $T = 5$:

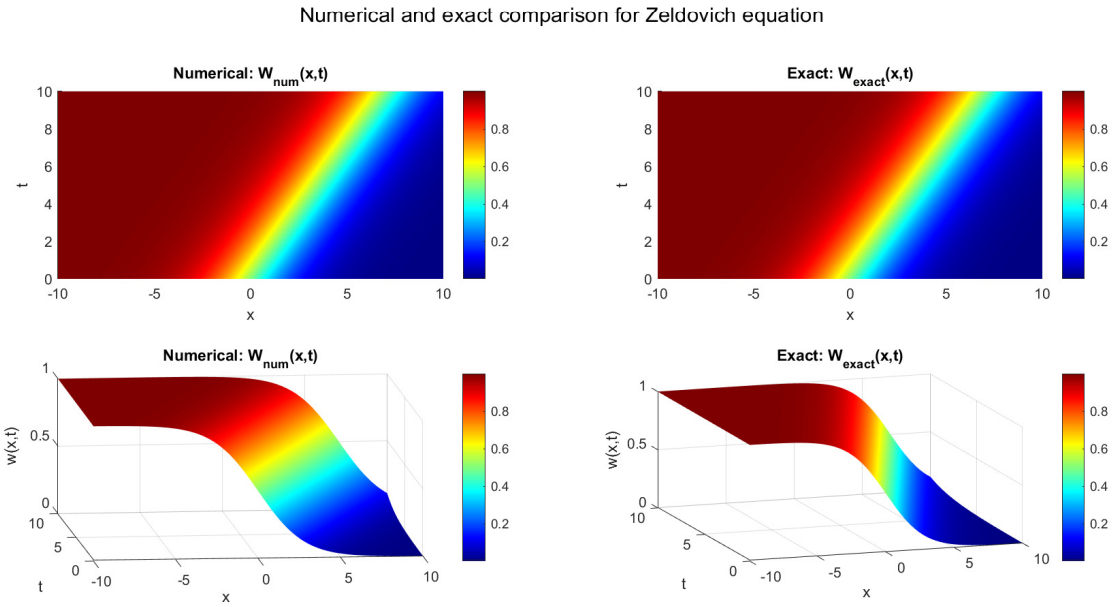

FIGURE 2. Surface plots in 2D and 3D showing the trade-off between the numerical and exact solutions for the Zeldovich model.

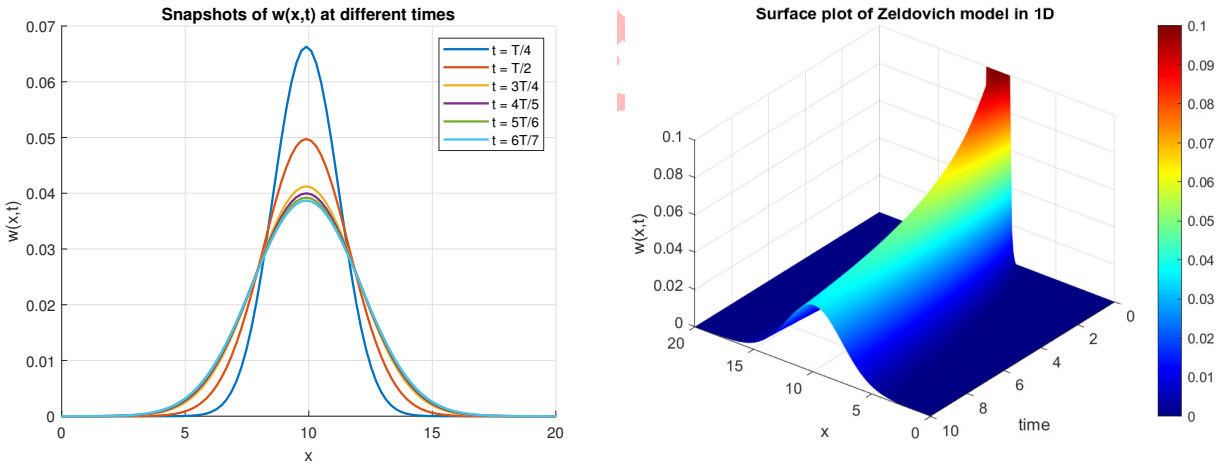

FIGURE 3. One-dimensional evolution of the Zeldovic model for $\alpha = 0.25, \beta = 0.5$ and $\gamma = 0.2$. Simulation runs for final time $T = 10$.

The central peak begins to spread as diffusion becomes more influential. The nonlinear reaction term starts to reduce the amplitude of w due to the negative cubic decay. When $T = 10$: The amplitude of the peak further decreases, and the bump spreads outward forming a shallow, circular wavefront. At $T = 15$: The solution continues to flatten out. Both diffusion and reaction contribute to suppressing any sharp features in the field. At $T = 20$: The field is almost homogeneous with low amplitude values across the domain. The central peak has dissipated significantly, and when $T = 25$: The system is near equilibrium with $w \approx 0$ everywhere, confirming the absorbing nature of the zero solution under the given dynamics.

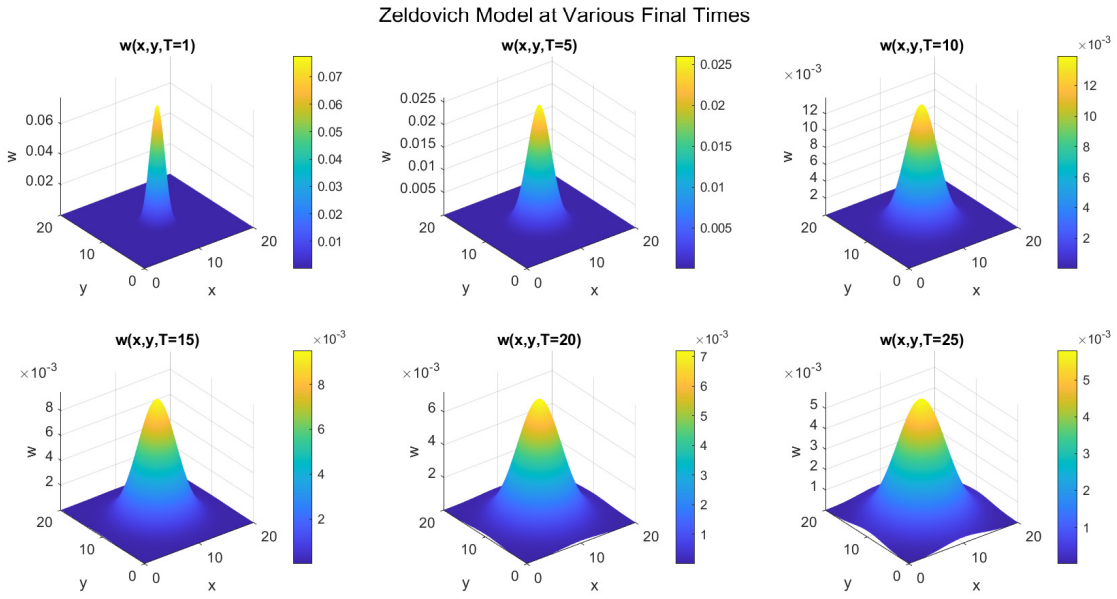

FIGURE 4. Surface plots of the solution $w(x, y, t)$ to the 2D Zeldovich model at various final times $T = 1, 5, 10, 15, 20, 25$. The initial condition is a localized perturbation centered in the domain. Over time, the solution exhibits smooth spreading due to diffusion and gradual decay due to the nonlinear reaction term. No sustained patterns or wavefronts form, and the system asymptotically approaches the homogeneous steady state $w = 0$.

The Zeldovich model combines reaction and diffusion processes typical of combustion theory, autocatalytic chemical reactions, and population dynamics with saturation effects. The term $-w^2(\beta + \gamma w)$ acts as a nonlinear sink, leading to self-limiting behavior even in the presence of spatial spreading via diffusion.

The simulations reveal that: The zero steady state is globally attractive for non-negative initial conditions. Any local perturbation, regardless of size, will eventually decay due to the dominance of the nonlinear damping term. There is no pattern formation or oscillatory dynamics; instead, the system exhibits monotonic decay toward equilibrium.

In practical contexts, such behavior can be interpreted as:

Combustion Quenching: A localized ignition will fail to sustain a flame unless external energy is continuously supplied. The reaction term models energy depletion, and diffusion alone cannot maintain the reaction front.

Population Collapse: In ecological systems with strong intraspecific competition (modeled by the cubic damping), any local increase in population will eventually decay if not supported by external resources or spatial influx.

Chemical Systems: In autocatalytic reactions with inhibitory feedback, even high initial concentrations may dissipate without a persistent energy or reactant source.

For the second case, we utilized the Matlab random initial condition and the zero-flux Neuman boundary conditions to examine the possibility of patterns in high-dimensional form of the Zeldovic equation. Specifically, we used $w = randn(N, N) * \epsilon$ where ϵ is a small noise. The 2D evolution of Zeldovich model is given in Figures 5 and 6. The Zeldovich model demonstrates how reaction–diffusion systems can exhibit stabilizing behaviors in contrast to more excitable or pattern-forming systems like the Gray-Scott or Brusselator models [15, 16].

So far, the proposed numerical scheme has been applied to both 1D and 2D Zeldovich equations, and the results are compared with exact solutions to validate the method. Extension of the scheme to 2D problem demonstrates the versatility and robustness of the scheme in higher dimensions, while maintaining the accuracy of the solutions.

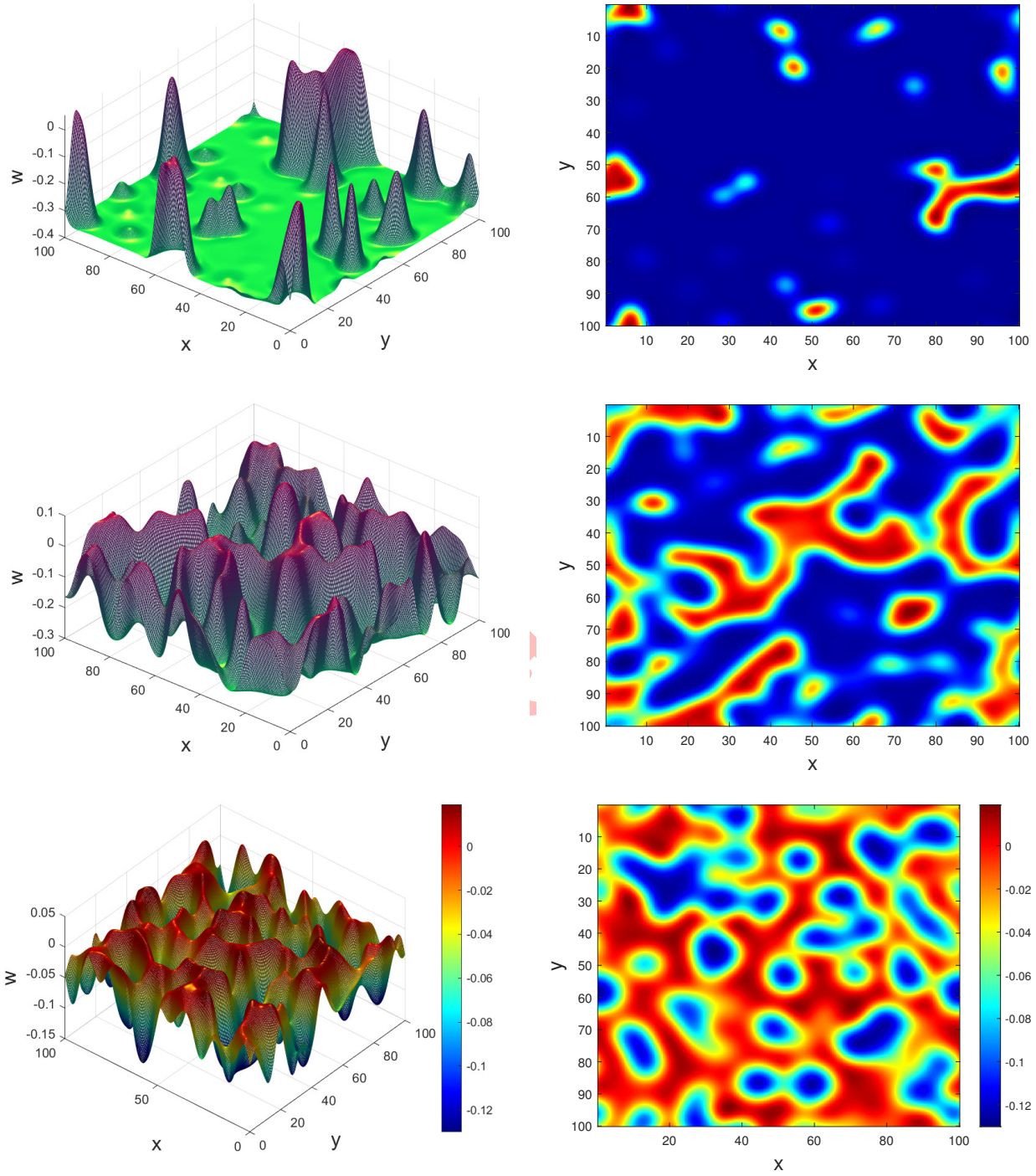

FIGURE 5. 2D evolution of the Zeldovic model for $\alpha = (0.25, 0.15, 0.1)\beta = 0.5$ and $\gamma = (2, 0.2, 0.1)$, showing chaotic-spiral spatial patterns.

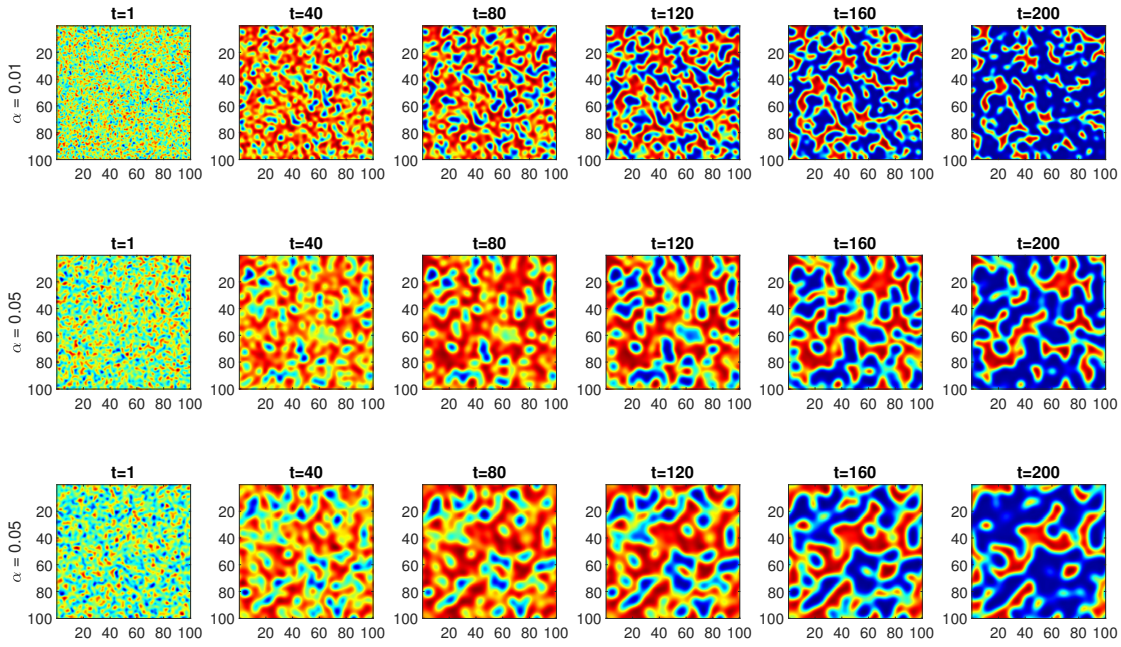

FIGURE 6. Surface plots 2D plots for Zeldovich model at various final times. Spatiotemporal and complex spiral waves is evident.

Extending to other practical problem. In addition to the Zeldovich equation, the numerical scheme is generalized to solve other relevant physical problems, such as the Fisher equation or Cahn-Hilliard equation, which models phase separation in binary mixtures. This demonstrates the capability of the method to tackle a broad range of practical problems in applied mathematics and computational physics.

By comparing with existing numerical methods, analyzing convergence rates, and evaluating the performance under various initial and boundary conditions, we show that the proposed scheme provides a highly accurate and efficient tool for solving nonlinear PDEs in both 1D and 2D.

For a typical example we consider the case of Fisher equation [13, 14]

$$\partial_t w = D w_{xx} + \tau w(1 - w/\kappa), \quad \tau > 0, \quad \kappa > 0, \quad D > 0, \tag{4.3}$$

in one-dimension, we compute the initial condition with a small perturbation at the center in the form $w = zeros(N, 1)$; $u(N/2 - 5 : N/2 + 5) = 0.1$ to obtain the solution in Figure 7 which shows the performance of the proposed schemes when compared with the exact equation, and the surface plot in Figure 8. showing the time evolution of the solution for the Fisher equation with different growth rates τ values as shown in the cation. The simulation experiment also extends to 2D as in Figure 9. Each subplot corresponds to one value of τ from the range $[0.25, 0.5, 0.75, 1.0, 1.25, 1.5]$. One can observe how the diffusion and growth dynamics change across different values of τ.

5. Conclusion

In this study, a hybrid numerical approach combining hyperbolic B-spline collocation with finite difference methods has been successfully developed and applied to the Zeldovich combustion model. The method utilizes fourth-order

hyperbolic polynomial B-spline basis functions within a collocation framework, along with Crank–Nicolson time discretization and Rubin–Graves linearization to handle nonlinearity. The scheme was proven to be stable via a rigorous von Neumann analysis and demonstrated favorable convergence behavior across a range of test problems. The accuracy and efficiency of the proposed method were validated through comparisons with an existing fourth-order finite difference scheme. The hybrid method consistently outperformed the reference method, as shown by lower error values in both L_2 and L_∞ norms. Moreover, the method was effectively extended to two-dimensional problems, capturing the spatiotemporal dynamics of the Zeldovich model with high fidelity.

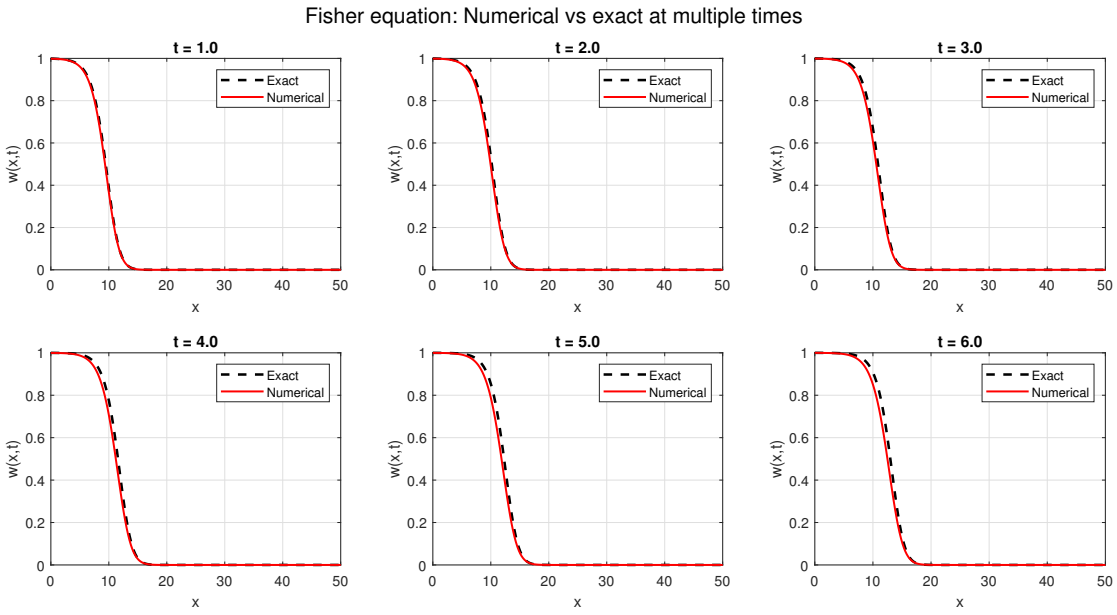

FIGURE 7. Accuracy test between the numerical and exact solutions when applied to solve Fisher equation in 1D.

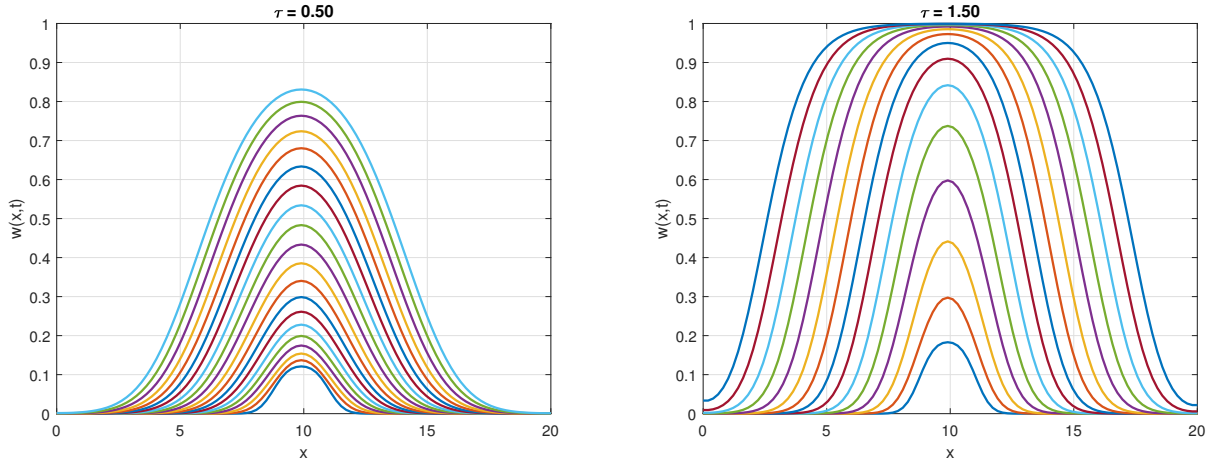

FIGURE 8. Traveling waves in 1D Fisher equation for different values of growth rate τ.

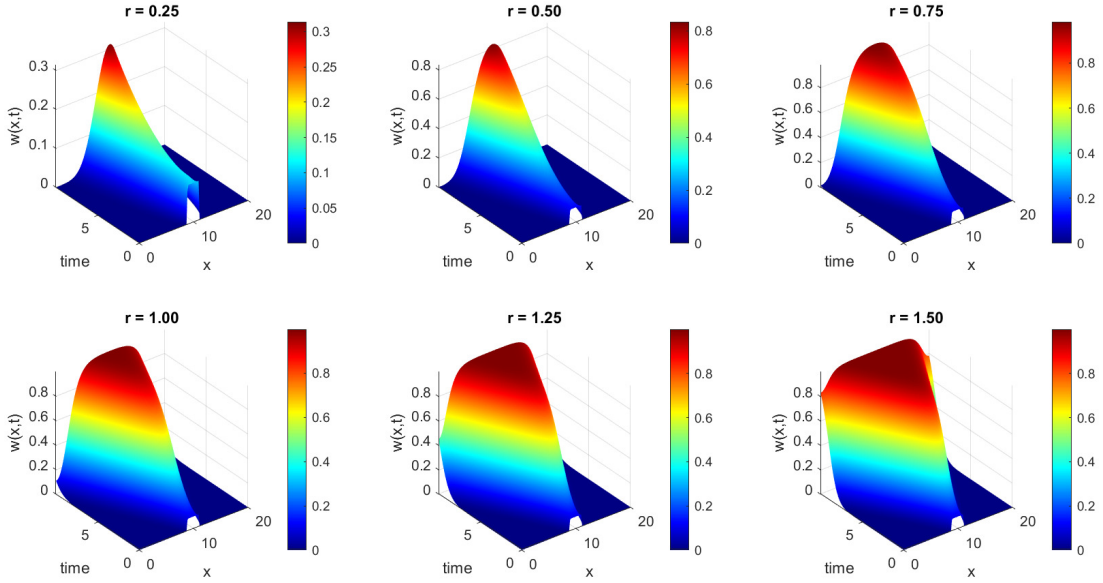

FIGURE 9. Dynamic evolution of Fisher equation in 2D for instances of growth rate τ at $t = 5$.

Beyond benchmark tests, the method was also applied to simulate the two-dimensional dynamics of the Zeldovich and Fisher equations. In both cases, it successfully reproduced intricate spatial spiral patterns, further demonstrating its capability to resolve complex reaction-diffusion phenomena. These results underscore the robustness and versatility of the hyperbolic B-spline collocation method and suggest its applicability to a broader class of nonlinear partial differential equations in combustion and biological systems.

ACKNOWLEDGMENT

Authors are thankful to the anonymous reviewers and the Editors in charge of our paper.

REFERENCES

[1] M. Abdelhakem, D. Abdelhamied, and Y. H. Youssri, *Two modified shifted Chebyshev–Galerkin operational matrix methods for even-order partial boundary value problems*. Boundary Value Problems, *2025*(1) (2025), 1-21.

[2] O. Abu Arqub, *Numerical solutions for the Robin time-fractional partial differential equations of heat and fluid flows based on the reproducing kernel algorithm*, International Journal of Numerical Methods for Heat & Fluid Flow, *28*(4) (2018), 828-856.

[3] O. Abu Arqub, *Numerical simulation of time-fractional partial differential equations arising in fluid flows via reproducing Kernel method*, International Journal of Numerical Methods for Heat and Fluid Flow, *30*(11) (2020), 4711-4733.

[4] O. Abu Arqub, and M. Al-Smadi, *Numerical solutions of Riesz fractional diffusion and advection-dispersion equations in porous media using iterative reproducing kernel algorithm*, Journal of Porous Media, *23*(8) (2020), 783-804.

[5] O. Abu Arqub, and N. T. Shawagfeh, *Application of reproducing kernel algorithm for solving Dirichlet time-fractional diffusion-Gordon types equations in porous media*, Journal of Porous Media, *22*(4) (2019), 411-434.

[6] M. S. Touati Brahim, Y. H. Youssri, A. Alburaikan, H. Khalifa, T. Radwan, and Ramy Hafez, *A refined Galerkin approach for solving higher-order differential equations via Bernoulli polynomials*, Fractals, (2025).

[7] S. Injrou, *Exact solutions for the conformable space-time fractional Zeldovich equation with time-dependent coefficients*, International Journal of Differential Equations, *2020*(1) (2020), 9312830.
[8] S. Injrou, *Finding various exact solutions for zeldovich equation in the sense of conformable fractional derivative with constant coefficients*, Tishreen University Journal for Research and Scientific Studies, *42*(3) (2020), 11-24.
[9] S. Injrou, *A Study about Finding Exact Solutions for Zeldovich Equation with Time-Dependent Coefficients by Using the Tanh Function Method*, Journal for Research and Scientific Studies-Basic Sciences Series, *40* (2018), 23-32.
[10] A. Korkmaz, Complex wave solutions to mathematical biology models I: Newell–Whitehead–Segel and Zeldovich equations, Journal of Computational and Nonlinear Dynamics, *13*(8) (2018), 081004.
[11] M. E. Munawer, *Human health and environmental impacts of coal combustion and post-combustion wastes*, Journal of Sustainable Mining, *17*(2) (2018), 87-96.
[12] J. G. Charney, R. Fjörtoft, and J. von Neumann, *Numerical integration of the Barotropic vorticity equation*, Tellus, *2*(4) (1950), 237-254.
[13] K. M. Owolabi, *Robust IMEX schemes for solving two-dimensional reaction- diffusion models*, International Journal of Nonlinear Science and Numerical Simulations, *16* (2015), 271-284.
[14] K. M. Owolabi and K. C. Patidar, *Solution of pattern waves for diffusive Fisher-like non-linear equations with adaptive methods*, International Journal of Nonlinear Sciences and Numerical Simulation, *17* (2016), 291-304.
[15] K. M. Owolabi, *Robust and adaptive techniques for numerical simulation of nonlinear partial differential equations of fractional order*, Communications in Nonlinear Science and Numerical Simulations, *44* (2017), 304-317.
[16] K. M. Owolabi and S. Jain, *Spatial patterns through diffusion-driven instability in modified predator–prey models with chaotic behaviors*, Chaos, Solitons and Fractals, *174* (2023), 113839.
[17] M. S. Palav and V. H. Pradhan, Redefined fourth order uniform hyperbolic polynomial B-splines based collocation method for solving advection-diffusion equation, Applied Mathematics and Computation, *484* (2025), 128992.
[18] K. Pikoñ *Environmental impact of combustion*, Applied Energy, *75*(3-4) (2003), 213-220.
[19] H. Ur Rehman, M. A. Imran, N. Ullah, and A. Akgul, *On solutions of the Newell–Whitehead–Segel equation and Zeldovich equation*, Mathematical Methods in the Applied Sciences, *44*(8) (2021), 7134-7149.
[20] S. G. Rubin and R. A. Graves, *A cubic spline approximation for problems in fluid mechanics*, National aeronautics and space administration, Technical Report, Washington, 1975.
[21] M. A. Taema and Y. H. Youssri, *Third-kind Chebyshev spectral collocation method for solving models of two interacting biological species*, Contemporary Mathematics, *5*(4) (2024), 6189-6207.
[22] Y. H. Youssri, L. A. Alnaser, and A. G. Atta, *A spectral collocation approach for time-fractional Korteweg–de Vries–Burgers equation via first-kind Chebyshev polynomials*, Contemporary Mathematics, *6*(2) (2025), 1501-1519.
[23] A. Yusuf, B. Ghanbari, S. Qureshi, M. Inc, and D. Baleanu, *Symmetry analysis and some new exact solutions of the Newell-Whitehead-Segel and Zeldovich equations*, Results in Nonlinear Analysis, *2*(4) (2019), 182-192.